ISSN 1318-0010
KZLTET 32(6)475(1998)

EFFECTS OF IMPURITIES IN ALLOY 800 ON THE GRAIN BOUNDARY DIFFUSION AND HIGH TEMPERATURE CREEP

VPLIV NEČISTOČ V ZLITINI 800 NA DIFUZIJO PO MEJAH ZRN IN NA VISOKO TEMPERATURNO LEZENJE

JANINE LINDEMANN, K. HENNESEN, C. DERDER, H. VIEFHAUS AND H. J. GRABKE

Max-Planck-Institut für Eisenforschung, Max-Planck-Str. 1, D-40237 Düsseldorf, Germany

Prejem rokopisa - received: 1998-09-21; sprejem za objavo - accepted for publication: 1998-12-14

Industrial Alloy 800 in different specifications and melts of Alloy 800 with addition of P and S were investigated using diffusion, segregation and creep measurements to reveal the influence of the impurities and to find relations between microstructure, creep properties and self-diffusivity. Using the radioactive tracer sectioning method the bulk and grain boundary diffusion of ^{59}Fe was determined in Alloy 800 in the temperature range 800 to 1000°C. In Alloy 800H the activation energy of grain boundary diffusion of ^{59}Fe is (209 ± 17) kJ/mol. The use of the approximation of Suzuoka was confirmed by autoradiographs. Dissolved elements especially P increase the activation energy of the grain boundary diffusion of Fe by their segregation to the grain boundaries and by increasing carbide precipitation at the grain boundaries. The same materials - aged at 800°C for 100 h - were used for creep experiments under constant load and constant temperature. The chemical composition of the creep cavities and grain boundaries were analysed by Auger Electron Spectroscopy (AES). For Alloy 800 + 0.09 wt-% P an enrichment of about 14 at-% P was observed at the grain boundaries. No correlation of creep cavity formation and diffusivity could be found. The addition of P clearly enhances the creep strength of Alloy 800; this can be explained by phosphides in the grains and by enhanced precipitation of $Cr_{23}C_6$ on the grain boundaries during the creep process.

Key words: alloy 800, grain boundary diffusion, solution of Suzuoka, sectioning method, radioactive tracer, residual activity, bulk diffusion, phosphorous, phosphides, sulphur, segregation, creep process, creep cavities, minimum creep strain rate

Raziskali smo difuzijo, segregacije in lezenje, da bi ugotovili vpliv nečistoč na mikrostrukturo, lastnosti lezenja in samodifuzijo v različnih industrijskih zlitinah 800 in v laboratorijsko izdelanih zlitin 800 z dodatkom P in S. Difuzija ^{59}Fe v osnovnem materialu in po mejah zrn v zlitini 800 je bila izmerjena z metodo radioaktivnih preiskav presekov, v temperaturnem področju od 800 do 1000°C. Za zlitino 800 H je aktivacijska energija difuzije ^{59}Fe po mejah zrn (209 ± 17) kJ/mol. Uporaba Suzouka aproksimacije je bila potrjena z avtoradiogrami. Raztopljeni elementi, posebno P zvišajo aktivacijsko energijo difuzije Fe po mejah zrn s tem, da segregirajo na meje zrn in zvišajo precipitacijo karbidov na mejah zrn. Enak material staran 100 ur na 800° C je bil uporabljen za eksperimente lezenja pod konstantno obremenitvijo in pri konstantni temperaturi. Kemijska sestava jamic nastalih pri lezenju in mej zrn je bila določena s Spektroskopijo na Augerjeve elektrone (AES). Pri zlitini 800 z 0.09 mas% P je bila izmerjena na mejah zrn obogatitev s 14 at.% P. Nobene povezave med difuzijo in tvorbo jamic pri lezenju ni bilo mogoče najti. Dodatek P jasno poveča odpornost Zlitine 800 proti lezenju; kar lahko razložimo s fosfidi v zrnih in s povečano precipitacijo $Cr_{23}C_6$ na mejah zrn med procesom lezenja.

Ključne besede: zlitina 800, difuzija po mejah zrn, Suzouka razlaga, metoda presekov, radioaktivne preiskave, rezidualna aktivnost, difuzija v osnovnem materialu, fosfor, fosfidi, žveplo, segregacije, procesi lezenja, jamice pri lezenju

1 INTRODUCTION

Alloy 800 is an austenitic iron-base alloy with 30 wt-% Ni and 20 wt-% Cr. It combines relatively high creep strength with good resistance against hot gas and combustion products as well as molten salts at temperatures above 550°C. Therefore, it is a preferred material for high-temperature applications in the chemical and petrochemical industry, when it is used for heat exchangers, piping systems and pyrolysis tubes. Alloy 800HT with a higher Ti-content and a higher but well-defined Al-content is the grade with the highest creep strength. Alloy 800LC, the low-carbon variant, exhibits excellent resistance against intergranular corrosion in aqueous media. Therefore, it is a standard material for steam generators and feedwater heaters in power stations. Under high stress conditions at high temperatures, a possible reason for failure of Alloy 800 is intergranular creep fracture initiated by the formation and growth of creep cavities. The formation of creep cavities is a diffusion controlled, thermally activated process. The cavities grow through grain boundary diffusion, surface diffusion or through dislocation creep in the vicinity of the creep cavities. The basic growth mechanism of cavities is probably the stress-directed diffusion of atoms away from the cavity into adjacent grain boundaries, where they are deposited. The linear growth rate $\partial R/\partial t$ of axisymmetric equilibrium cavities is direct proportional to the grain boundary diffusion coefficients $\delta \cdot D_{gb}$[1]. Therefore, not only the creep behaviour of Alloy 800, but also the grain boundary diffusion was investigated and grain boundary diffusion coefficients were calculated.

2 MATERIAL PREPARATION AND EXPERIMENTAL SETUP

The three industrial specifications of Alloy 800 have been investigated, and in addition further melts contain-

Table 1: Chemical composition (wt-%) of the investigated materials (Fe: remainder) and the obtained grain sizes (μm)

	Ni	Cr	Ti	Al	C	P	S	Mn	Grain sizes
Alloy 800H	30.2	19.7	0.34	0.29	0.074	0.010	<0.001	0.78	90-110
Alloy 800HT	30.4	19.6	0.51	0.45	0.090	0.010	<0.001	0.73	110-130
Alloy 800LC	32.1	19.9	0.48	0.31	0.016	0.017	0.004	0.69	70-90
Alloy 800+P	29.8	19.6	0.35	0.30	0.069	0.088	0.002	0.70	35-45
Alloy 800+S	29.7	19.7	0.35	0.30	0.069	0.014	0.041	0.70	35-45

ing P or S were prepared and studied. The chemical composition of the materials is shown in **Table 1**. Recrystallization annealing was conducted at 1150°C for 30 min with a subsequent water quenching. For the stabilisation of the grain sizes and to reach equilibrium segregation, the materials were aged at 800°C for 100 h; the obtained grain sizes are also listed in **Table 1**. From these materials samples were prepared for diffusion, segregation and creep measurements.

For diffusion measurements cylindrical samples (ϕ = 11.9 mm, h = 4.0 mm) were coated electrolytically from an $FeCl_2$ solution containing the radioactive tracer ^{59}Fe resulting in a 0.2 μm iron layer. After the diffusion annealing thin layers of the specimens were successively abraded and the residual activity was determined to obtain penetration profiles of the tracer.

Auger-measurements were carried out on fracture samples to check if grain boundary segregation of elements takes place. Cylindrical notched specimens were cooled to about -120°C, then fractured by impact in the UHV chamber of the spectrometer and analysed on intergranular fracture facets.

Creep experiments were carried out using 20 kN and 30 kN testing machines; temperature constancy was ensured for 5 cm more than the sample length in the three-zone-controlled furnace. Creep measurements were carried out in air at constant temperature (800°C) with constant load (σ = 100 MPa, 80 MPa, 60 MPa) and heating times according to DIN 50118. The creep samples were prepared according to DIN 50118 from the aged materials.

After creep rupture the stressed parts of the creep samples, especially the creep cavities were analysed by AES and by scanning Auger mapping (SAM). Furthermore, the precipitates in the deformed creep samples were investigated by transmission electron microscopy (TEM).

3 RESULTS AND DISCUSSION

a) Diffusion measurements

The diffusion samples (6 each under the same conditions) were diffusion annealed under argon in the temperature range of 800 to 1000°C for periods between 100 and 2 days **(Table 2)**. The exposure time was chosen to be sufficient to determine the bulk and grain boundary diffusivities in the same experiments and to fulfil the limiting conditions of the kinetic B regime[2,3].

After diffusion annealing the penetration profile of Fe^{59} was determined by successive abrasions of thin layers in combination with residual activity measurements. The residual activity β-counts of the diffusion samples can be related to the tracer concentration in the given layer using the approximation of Borg and Birchenall[4]. To distinguish between volume and grain boundary diffusion regions autoradiographs were taken in different penetration depths. A depletion of the radiotracer above the grain boundaries was observed[5]. To obtain grain boundary coefficients D_{gb} from the penetration profiles the approximation of Suzuoka[6,7] was used; this evaluation method considers the depletion of the tracer on the surface.

The measured grain boundary coefficients $P = k \cdot \delta \cdot D_{gb}$ (k: segregation factor; δ = 0.5 nm grain boundary width) for Fe in Alloy 800 are plotted in **Figure 1a,b** as Arrhenius-plots. The following relations were determined for the triple product P:

Alloy 800H $P(cm^3s^{-1})$=
$=(3.1\pm1.8)\cdot10^{-5}\ cm^3s^{-1}\cdot\exp(-(209\pm17)kJ\cdot mol^{-1}/RT)$

Alloy 800HT $P(cm^3s^{-1})$=
$=(8.9\pm4.2)\cdot10^{-5}\ cm^3s^{-1}\cdot\exp(-(221\pm14)kJ\cdot mol^{-1}/RT)$

Alloy 800LC $P(cm^3s^{-1})$=
$=(1.3\pm0.5)\cdot10^{-5}\ cm^3s^{-1}\cdot\exp(-(194\pm11)kJ\cdot mol^{-1}/RT)$

Alloy 800+S $P(cm^3s^{-1})$=
$=(9.9\pm2.4)\cdot10^{-4}\ cm^3s^{-1}\cdot\exp(-(242\pm7)kJ\cdot mol^{-1}/RT)$

Alloy 800+P $P(cm^3s^{-1})$=
$=(9.8\pm7.3)\cdot10^{-2}\ cm^3s^{-1}\cdot\exp(-(288\pm22)kJ\cdot mol^{-1}/RT)$

The diffusion coefficients of Fe in Alloy 800 are in close agreement with measurements in similar Fe-Ni-Cr alloys[8]. The dissolved elements P, S and C increase the activation energy of grain boundary diffusion of Fe and so delay the grain boundary diffusion in Alloy 800 at least in the low temperature range. This can be explained by the grain boundary segregation of the dissolved elements, they occupy the high energy sites with high diffusivities at the grain boundaries. Besides, the impurities enhance the formation of carbide precipitates at the grain boundaries, which also reduces the mobility of Fe in the short circuit paths.

The relatively high activation energy in undoped Alloy 800 is caused by the high C-content, as can be concluded, since the same value was obtained for measurements in α-iron doped 140 ppm C[9]. Comparing the activation energies of the grain boundary self-diffusion in Alloy 800 and in α-Fe[9] it is clear that the influence of the dissolved elements is similar **(Table 3)**.

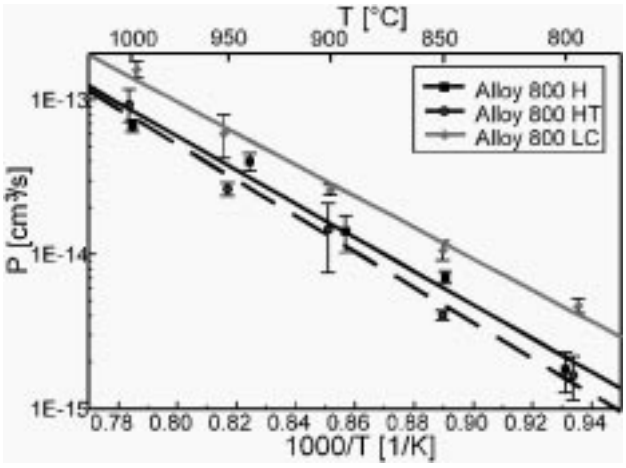

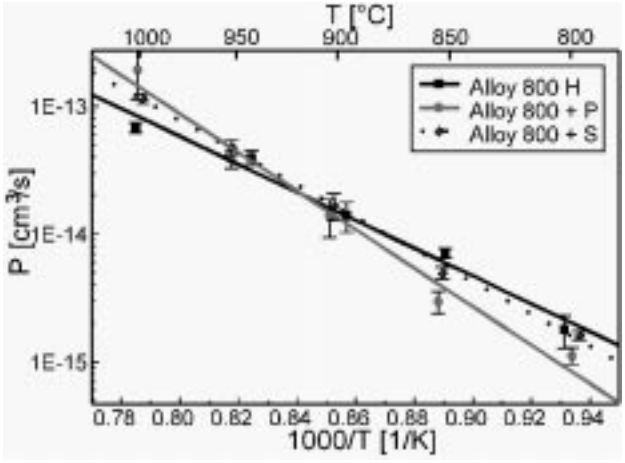

Figure 1a: Arrhenius-plot of grain boundary diffusion coefficients of Fe in Alloy 800H, Alloy 800HT and Alloy 800LC
Figure 1b: Arrhenius-plot of grain boundary diffusion coefficients of Fe in Alloy 800H, Alloy 800+P and Alloy 800+S
Slika 1a: Arrheniusov diagram difuzijskega koeficienta Fe po mejah zrn v zlitinah 800H, 800HT in 800LC
Slika 1b: Arrheniusov diagram difuzijskega koeficienta Fe po mejah zrn v zlitinah 800H, 800+P in 800+S

b) Segregation measurements

Surface active elements should influence the grain boundary diffusion of Fe in two ways. They vary the activation energy for interchange of sites and they tie up the Fe atoms at the grain boundaries. Therefore, grain boundary diffusion coefficients are decreased by the segregation factor k: $P=k\cdot\delta\cdot D_{gb}$.

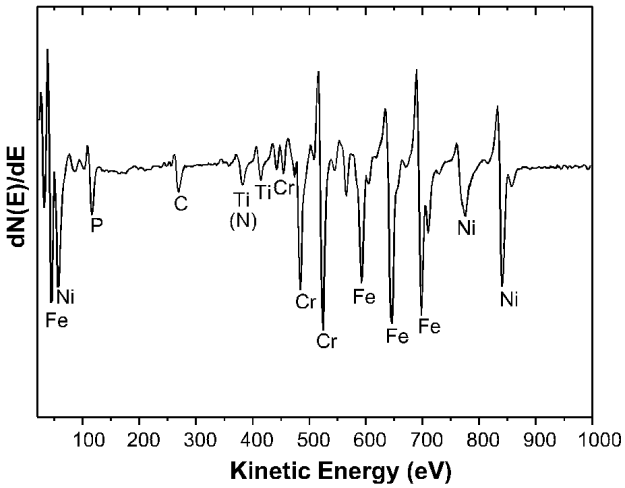

Figure 2: Auger-analysis of an intergranular facet in Alloy 800 + 0.09 wt-% P
Slika 2: AES spekter na interkristalni faseti v zlitini 800 + 0.09 mas% P

Table 2: Diffusion times

	t_{diff} (days)				
	800°C	850°C	900°C	950°C	1000°C
Alloy 800H	100	75	54	11	4
Alloy 800HT	96	75	55	11	4
Alloy 800LC	98	55	30	11	4
Alloy 800+P	98	39	22	11	4
Alloy 800+S	86	69	22	4	2

Analysing the five materials, dimpled fracture was observed exclusively in Alloy 800LC and predominantly in Alloy 800H and HT; any possible enrichment at the grain boundaries cannot be observed in these alloys. Alloy 800+P shows mainly intergranular fracture **(Figure 4)**; Auger spectra taken on the grain surfaces clearly demonstrate the enrichment of P **(Figure 2)**. The P-concentration at the grain boundaries is in the range of 14 at-% of a monolayer. In Alloy 800+S both intergranular fracture and dimpled fracture was found. **Figure 3** shows an enrichment of Ti, S and C with constant peak-to-peak-height-ratio at different analysed locations; by

Table 3: Comparison of the grain boundary-activation energies in Alloy 800 and α-Fe[9]

Material	C (wt-ppm)	Ti (wt-%)	S (wt-ppm)	P- (wt-ppm)	α-Fe E_A(kJ/mol)	Alloy 800 E_A(kJ/mol)
α-Fe,pure	27	0.055	/	/	105±20	
Alloy 800H	740	0.340	/	/		209±17
α-Fe+C	140	0.025	/	/	185±18	
Alloy 800LC	160	0.480	/	/		194±11
Alloy 800HT	900	0.510	/	/		221±14
α-Fe+P	21	0.007	/	1700	201±15	
Alloy 800+P	690	0.350	/	880		288±22
α-Fe+S	15	0.007	120	/	177±18	
Alloy 800+S	690	0.350	410	/		242±7

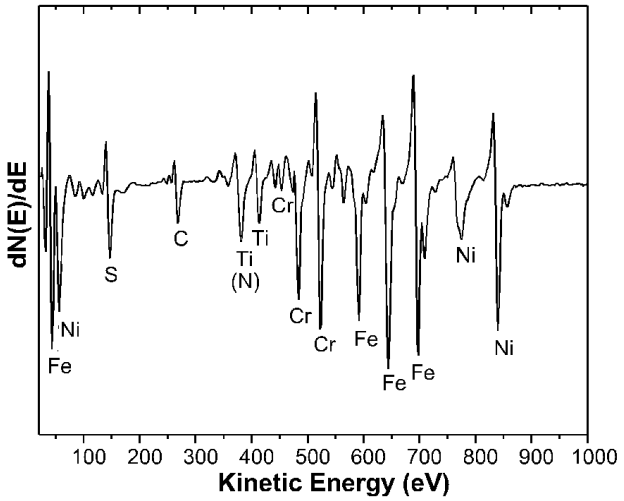

Figure 3: Auger-analysis of a grain boundary in Alloy 800 + 0.04 wt-% S
Slika 3: AES spekter na meji zrn v zlitini 800 + 0.04 mas% S

TEM/EDX measurements and diffraction pattern these enrichments were identified as precipitation of $Ti_4S_2C_2$ and of TiS **(Figure 5)**.

b) Creep measurements

Creep experiments were conducted at constant temperature (800°C) under constant load (σ = 60, 80, 100 MPa) using creep samples prepared according to DIN 50118.

The most interesting result of the creep experiments is the influence of P. In the literature, there is no uniform

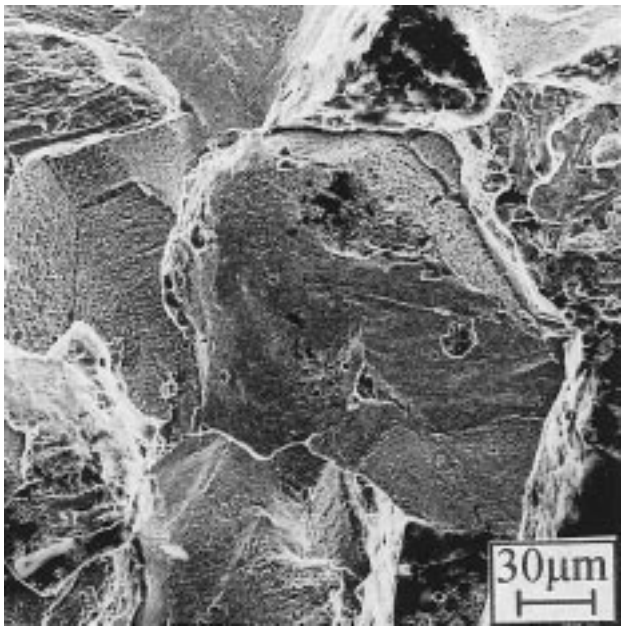

Figure 4: SEM of a typical intergranular fracture in Alloy 800 + 0.09 wt-% P
Slika 4: SEM posnetek značilnega interkristalnega preloma v zlitini 800 + 0.09 mas% P

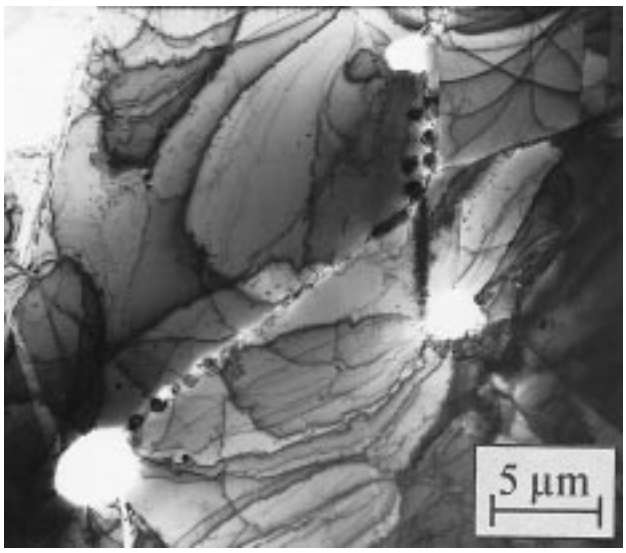

Figure 5: $Ti_4C_2S_2$-precipitation at grain boundary facet in Alloy 800 + 0.04 wt-% S; TEM (bright field)
Slika 5: TEM posnetek $Ti_4C_2S_2$ precipitatov na faseti na meji zrn v zlitini 800 + 0.04 mas% S (svetlo polje)

opinion about the influence of P on the creep strength. Jäger[10] has observed that Sn and P together decrease the creep strength of iron base alloys. Gärtner[11] has found a positive influence of P on creep strength of Nimonic 80A, but a negative influence on nickel. A possible explanation for the positive influence of P on Nimonic 80A was found to be an additional precipitation of $Cr_{23}C_6$ on grain boundaries during the creep process, because P reduces the grain boundary concentration of C and enhances the precipitation of these carbides. Nishimura[12] has investigated the influence of P on 9Cr-1Mo steel under two different conditions: a) 147 MPa at 600°C and b) 90 MPa at 650°C. He observed at 147 MPa an increase of creep strength for a higher amount of P, but at 90 MPa a decrease of creep strength with increasing P-content.

Our creep experiments showed that the addition of P clearly enhances the creep strength of Alloy 800 for all stresses. Phosphorous decreases the minimum creep strain rates up to two orders of magnitude, enhances the creep rupture time **(Figure 6a,b)**, and decreases the creep rupture strain **(Table 4, Figure 7)**. After creep rupture the samples were analysed by AES and TEM. Addition of P reduces the creep cavity formation; in the creep cavities and at the grain boundaries in Alloy 800+P $Cr_{23}C_6$-precipitates and P-segregation were observed. By the fcc-structure of the $Cr_{23}C_6$ precipitates at the grain boundaries the coherence to the matrix seems to be increased. This observation corresponds to the results of Gärtner[11].

However, an influence of P on creep strain of two orders of magnitude is too strong than to be explained just as a grain boundary effect. TEM-measurements showed precipitation of platelet phosphides in the matrix **(Figure 8)** in addition to TiC, TiN and $Cr_{23}C_6$, which are found in

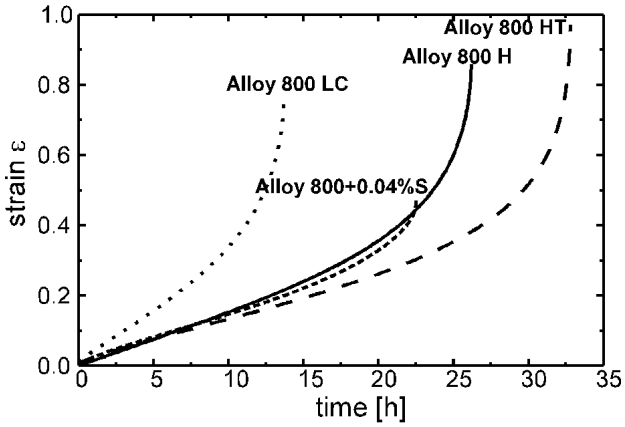

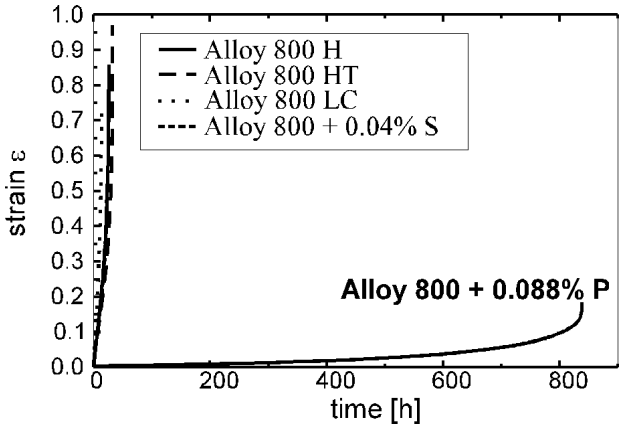

Figure 6a: Creep strain plots at 800°C and σ = 80 MPa of Alloy 800H, HT, LC and Alloy 800+0.04% S

Figure 6b: Creep strain plots at 800°C and σ = 80 MPa of Alloy 800+0.09% P in comparison to other Alloy 800 specifications

Slika 6a: Diagram napetosti lezenja pri 800°C in σ = 80 MPa zlitina 800H, HT, LC in zlitina 800+0.04 mas% S

Slika 6b: Diagram napetosti lezenja pri 800°C in σ = 80 MPa zlitina 800+0.09 mas % P in primerjava z različnimi zlitinami 800

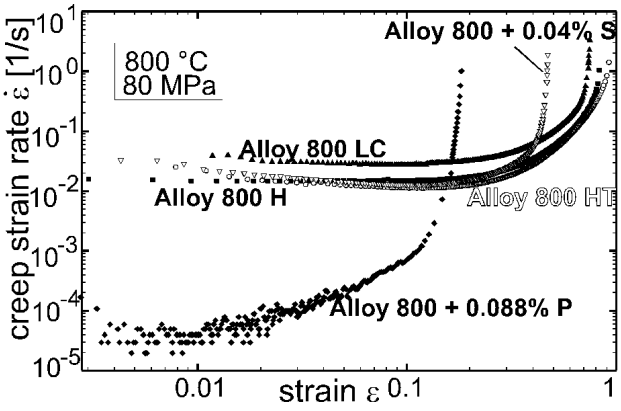

Figure 7: Creep strain rates of Alloy 800 at 800°C and σ = 80 MPa

Slika 7: Stopnje napetosti lezenja za zlitino 800 pri 800°C in σ = 800 MPa

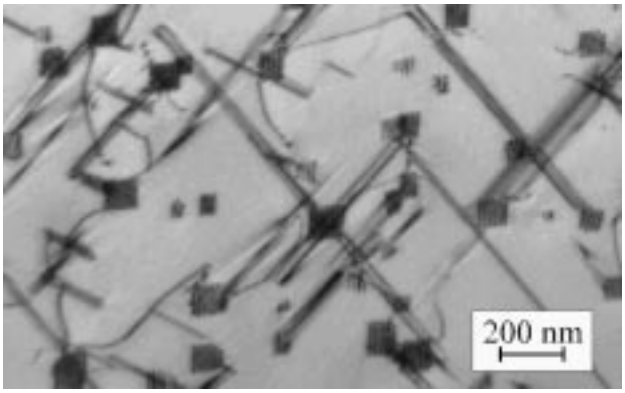

Figure 8: Precipitates (platelets phosphides) in Alloy 800 + 0.09 wt% P; TEM (bright field)

Slika 8: TEM posnetek precipitatov (ploščice fosfidov) v zlitini 800 + 0.09 mas% P

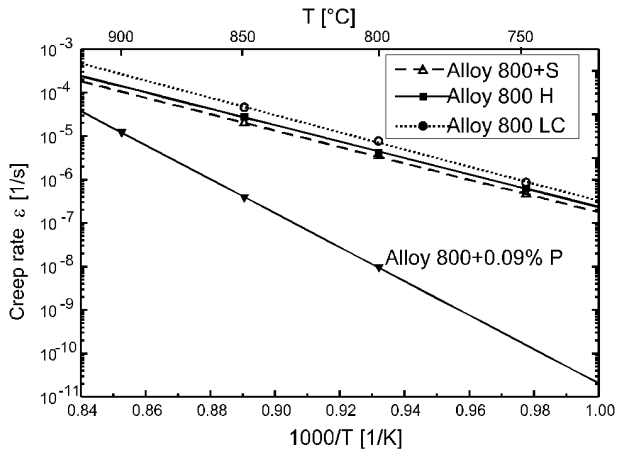

Figure 9: Arrhenius-plot of minimum creep strain rates of Alloy 800 at σ = 80 MPa

Slika 9: Arrheniusov diagram minimalne stopnje napetosti lezenja zlitine 800 pri σ = 80 MPa

Alloy 800. These platelet phosphides may be the main reason for the better creep strength of Alloy 800+P, they impede the climbing of dislocations.

Another aspect of the investigation are the creep cavities. Alloy 800+P is the investigated material with the less of creep cavities. In contrast, in Alloy 800+S much more creep cavities than in Alloy 800 were observed. Therefore, the correlation between creep cavity formation and grain boundary self-diffusion could not be confirmed: both, P and S, increase the activation energy of grain boundary diffusion of Fe in Alloy 800, but P decreases creep cavity formation and S enhances creep cavity formation. As mentioned, P-segregation to the creep cavities in Alloy 800+P was found by AES, but in the creep cavities of the other materials no enrichment of any element was observed.

Further creep experiments under constant load (σ = 80 MPa) and at different constant temperatures (750°C, 800°C, 850°C and 900°C) are in progress. First results are shown in **Figure 9** as Arrhenius-plots of the minimum creep strain rates. It can be seen, that there is no

difference between the creep activation energies of Alloy 800H, LC and also Alloy 800 + 0.04% S, they are in the range of (156 ± 8) kJ/mol. In contrast, the addition of P increases the activation energy of creep up to the range of 325 kJ/mol.

Table 4: Minimum creep strain rates ε'_{min} [1/s] obtained at 800°C and different stresses σ

	Alloy 800H	Alloy 800HT	Alloy 800LC	Alloy 800+S	Alloy 800+P
σ=100 MPa	1.8 E-05	1.5 E-05	3.0 E-05	1.4 E-05	1.3 E-07
σ= 80 MPa	4.2 E-06	3.1 E-06	7.8 E-06	3.5 E-06	9.7 E-09
σ= 60 MPa	2.8 E-07	3.1 E-07	1.4 E-06	3.9 E-07	2.8 E-09

4 CONCLUSIONS

S and especially P enhance the activation energy of grain boundary diffusion of Fe in Alloy 800. In Alloy 800+S this is due to precipitation of $Ti_4S_2C_2$ and TiS at the grain boundaries. In Alloy 800+P, P segregates to the grain boundaries and $Cr_{23}C_6$ precipitates at the grain boundaries.

Addition of P clearly enhances the creep strength. This is due to the fcc-structured $Cr_{23}C_6$ precipitation at the grain boundaries and due to precipitation of phosphides in the matrix.

No connection between grain boundary diffusion and creep cavity formation could be observed; addition of S enhances and P reduces the creep cavity formation.

5 REFERENCES

[1] H. Riedel; *Fracture at High Temperatures, Material Research and Engineering*, Springer-Verlag Berlin (1987) 152

[2] I. Kaur, Y. Mishin, W. Gust; *Fundamentals of Grain and Interphase Boundary Diffusion*, Third enlarged edition, John Wiley & Sons Ltd 1995

[3] L. G. Harrison; *Trans. Faraday Soc.*, 57 (1961) 1191

[4] R. J. Borg, C. Birchenall, *Trans. Met. Soc. AIME*, 218 (1960) 980

[5] J. Lindemann, K. Hennesen, R. Mast, H. Viefhaus, H. J. Grabke; *Proceedings NIM Münster*, March 1998, GDMB Clausthal-Zellerfeld (1998) 115

[6] T. Suzuoka, *J. Phys. Soc. of Japan*, 19 (1964) 839

[7] T. Suzuoka, *Trans. Jap. Inst. Met.*, 2 (1961) 25

[8] J. Rothman, L. J. Nowicki, G. E. Murch; *J. Phys. F*, 10 (1980) 3, 383

[9] H. Hänsel, L. Stratmann, H. Keller, H. J. Grabke; *Acta Met.*, 33 (1985) 659

[10] W. Jäger, H. J. Grabke, J. Yu, *Proc. 2nd Int. Conf. on Creep and Fracture Engineering Materials and Structures*, 1986, Swansea, Ed. B. Wilshire, D. R. J. Owen

[11] E. Gärtner, H. J. Grabke, *Mat. Sci. Technology*, 9 (1993) 295

[12] N. Nishimura, M. Ozaki, F. Musuyama, *Proc. Clean Steels 5*, Balatonfüred, (1997) 117